Soil Biology and Biochemistry 118 (2018) 8–17

Contents lists available at ScienceDirect

Soil Biology and Biochemistry

journal homepage: www.elsevier.com/locate/soilbio

Ralstonia solanacearum pathogen disrupts bacterial rhizosphere microbiome during an invasion

Zhong Wei[a], Jie Hu[a,b], Yi'an Gu[a], Shixue Yin[c], Yangchun Xu[a,*], Alexandre Jousset[a,b], Qirong Shen[a], Ville-Petri Friman[d]

[a] Jiangsu Provincial Key Lab for Organic Solid Waste Utilization, Jiangsu Collaborative Innovation Center for Solid Organic Waste Resource Utilization, National Engineering Research Center for Organic-based Fertilizers, Nanjing Agricultural University, Weigang 1, Nanjing 210095, PR China
[b] Institute for Environmental Biology, Ecology & Biodiversity, Utrecht University, Padualaan 8, 3584CH Utrecht, The Netherlands
[c] College of Environmental Science and Engineering, Yangzhou University, Yangzhou, Jiangsu Province 225127, PR China
[d] University of York, Department of Biology, Wentworth Way, York YO10 5DD, UK

ARTICLE INFO

Keywords:
Bacterial wilt
Community ecology
Invasion resistance
Ecosystem functioning microbial interaction networks
Ralstonia solanacearum

ABSTRACT

Plant pathogen invasions are often associated with changes in physical environmental conditions and the composition of host-associated rhizosphere microbiome. It is however unclear how these factors interact and correlate with each other in determining plant disease dynamics in natural field conditions. To study this, we temporally sampled the rhizosphere of tomato plants that were exposed to moderate to aggressive *Ralstonia solanacearum* pathogen invasions over one crop season. We found that physiochemical soil properties correlated weakly with the severity of pathogen invasion apart from the water-soluble nitrogen concentration, which increased more clearly during the aggressive invasion. Instead, a much stronger link was found between pathogen invasion and reduced abundance and diversity of various rhizosphere bacterial taxa, simplification of bacterial interaction networks and loss of several predicted functional genes. We further verified our results in a separate greenhouse experiment to show that pathogen invasion causally drives similar changes in rhizosphere microbiome diversity and composition under controlled environmental conditions. Our results suggest that *R. solanacearum* invasion disrupts rhizosphere bacterial communities leading to clear reduction in the diversity and abundance of non-pathogenic bacteria. These changes could potentially affect the likelihood of secondary pathogen invasions during following crop seasons as less diverse microbial communities are also often less resistant to invasions. Strong negative correlation between pathogen and non-pathogenic bacterial densities further suggest that relative pathogen abundance could better predict the severity of bacterial wilt disease outbreaks compared to absolute pathogen abundance. Monitoring the dynamics of whole microbiomes could thus open new avenues for more accurate disease diagnostics in the future.

1. Introduction

Understanding plant pathogen infections in highly variable field conditions is a key challenge for crop protection and future food security. Specifically, it has remained difficult to disentangle the interactive and causal effects between abiotic environmental conditions, soil physiochemical properties, plant development and microbe-microbe interactions under variable field conditions (Chaparro et al., 2014; Huang et al., 2013; Li et al., 2013; Shi et al., 2015; Wei et al., 2011). In the case of *Ralstonia solanacearum* bacterial pathogen, both abiotic and biotic factors have been shown to be important for the infection dynamics (van Elsas et al., 2001; Wei et al., 2011). On a seasonal scale, disease outbreaks have been connected to periods of warm temperatures during the summer crop seasons (Wei et al., 2017, 2011), whereas at more local scale, *R. solanacearum* survival has been linked to low environmental salt concentration and water temperature (Elsas et al., 2001). Also other physiochemical soil properties vary spatially and temporally due to environmental heterogeneity and along with plant development and this variation could be important in explaining the patchiness of bacterial disease dynamics in homogenous agricultural monocultures (Piotrowska-Dlugosz et al., 2016).

In addition to abiotic environmental factors, biotic interactions can affect *R. solanacearum* infection dynamics via resource and interference competition within the host-associated rhizosphere bacterial communities (Wei et al., 2015). For example, microbial community composition and diversity (Chapelle et al., 2016; Elsas et al., 2012; Mendes

* Corresponding author.
E-mail address: ycxu@njau.edu.cn (Y. Xu).

https://doi.org/10.1016/j.soilbio.2017.11.012
Received 7 July 2017; Received in revised form 11 November 2017; Accepted 18 November 2017
Available online 06 December 2017
0038-0717/

et al., 2011), secondary metabolite activity (Jousset et al., 2014; Wang et al., 2017a), and interaction network architecture (Wei et al., 2015) have been connected to *R. solanacearum* pathogen invasions. Recent evidence also suggests that microbial interactions in the plant rhizosphere can be highly dynamic and shaped by plant development and abiotic environmental conditions (Gu et al., 2016; Wei et al., 2017). For example, plant exudation can change the rhizosphere community composition by recruiting certain beneficial microbes and directly repelling the pathogen (Wei et al., 2017), whereas nutrient availability and temperature has been shown to alleviate diversity-invasion resistance relationships via resource competition (Mallon et al., 2015), and to regulate competitive outcomes between the pathogen and endophytic biocontrol bacterium within the plant stem (Wei et al., 2017), respectively. As a result, disentangling the relative importance of multiple abiotic and biotic factors for pathogen invasion remains a key challenge for understanding the epidemiology of diseases. Here we studied this specifically in the context of *Ralstonia solanacearum* plant bacterial pathogen infecting tomato plants under natural field conditions in China.

Ralstonia solanacearum is a gram-negative plant pathogenic bacterium and a causal driver of global bacterial wilt disease epidemics (Hayward, 1991; Jiang et al., 2017; Yabuuchi et al., 1995). It has an unusually wide host range being capable of infecting more than 200 plant species including many economically important crops (Genin and Denny, 2012; Hayward, 1991; Jiang et al., 2017). The first step of infection is colonization of the plant rhizosphere, where the pathogen must compete with other bacterial taxa (Hibbing et al., 2010). After reaching a threshold density, pathogen switches on its virulence gene expression and invades plant roots (Schell, 2000). Once within xylem vessels, *R. solanacearum* rapidly spreads to aerial plant parts throughout the vascular system (Dalsing et al., 2015; Huang and Allen, 2000; Saile et al., 1997) and blocks the water flow via excessive production of extracellular polysaccharides (Denny and Baek, 1991; Genin and Denny, 2012). Bacterial wilt disease dynamics are often very variable in even seemingly homogenous agricultural monocultures, which raises a question: to what extent does abiotic and biotic environmental factors determine the epidemiology of bacterial wilt? To study this in more detail, we set up a temporal sampling regime where we repeatedly isolated the whole bacterial communities from tomato plant rhizosphere during a Spring crop season in Nanjing, China. Total pathogen and bacterial densities and the soil physiochemical properties (pH, water-soluble carbon, water-soluble nitrogen, nitrate, ammonium and available phosphate) were determined at every sampling and high-throughput sequencing used to determine changes in the rhizosphere bacterial community composition, co-occurrence interaction networks and changes in functional gene abundances with PICRUSt platform (Langille et al., 2013). We then explored the causal effect of pathogen invasion on rhizosphere microbiome composition in separate greenhouse experiment in controlled environmental conditions. We set to study following two key hypotheses: 1) does soil physiochemical properties and rhizosphere microbiome community composition correlate with the aggressiveness of pathogen invasions, and, 2) does the aggressiveness of pathogen invasion affect the diversity and functioning of rhizosphere microbiome communities?

2. Materials and methods

2.1. Experimental field site and sampling regime

The field experiment was conducted in Qilin town (118°57′E, 32°03′N), a vegetable production centre for the nearby urban population of Nanjing city, China. The experimental field has been continuously colonized by *R. solanacearum* for more than 10 years (Wei et al., 2011), and hence, bacterial wilt infection will occur naturally during the crop seasons. For this study, we selected one large field (~360 m^2 area) with very high disease incidence of bacterial wilt of tomato (~60% disease incidence during 2012 Autumn crop season) for field sampling during 2013 Spring crop season (from March to June).

Surface-sterilized tomato seeds (*Lycopersicon esculentum*, cultivar "Jiangshu") were germinated on water-agar plates for three days before sowing into seedling plates containing Cobalt-60-sterilized seedling substrate (Huainong, Huaian soil and fertilizer Institute, Huaian, China). On March 14th of 2013, thirty-day aged tomato seedlings were transplanted in the field (~2000 plants transplanted in the beginning of the crop season) and weekly sampling regime started ten days after the transplantation. For the first three weeks, nine healthy plants were randomly collected per week as no visible disease symptoms could be detected. From week four on, tomato plants started to show symptoms of wilting and approximately 50% of plants showed clear signs of bacterial wilt by the end of the crop season (Figs. S1–A). As a result, 6 healthy and 6 diseased plants were randomly collected from week 4 on and only plants with functional root systems were used for further analysis (Figs. S1–B). Sampling was finished 12 weeks after the transplantation.

Samples were classified into three groups based on the sampling time and visibility of bacterial wilt disease symptoms. Samples collected during the first 3 weeks were categorized to the group of initially healthy plants. From week four on, samples were categorized into two groups based on the visibility of bacterial wilt disease symptoms: healthy (no clear disease symptoms regardless of the pathogen presence) and diseased (clear diseases symptoms and high pathogen densities) plants. This classification was used because *R. solanacearum* was also present in the rhizosphere of the healthy plants even though it was not causing visible disease symptoms. Total of 112 rhizosphere soil samples were collected during the 12-week crop season resulting in 27 initial, 35 diseased and 50 healthy plant rhizosphere samples. The following physiochemical soil properties were also measured from each field sample: pH (1: 5 mass ratio of sample and deionized water, PB-10, Sartorius, Germany) (Li et al., 2017), nitrate and ammonium nitrogen (AutoAnalyzer 3, SEAL, Germany), and water-soluble nitrogen and carbon concentrations (Vario TOC cube, Elementary, Germany).

2.2. Greenhouse experiment testing for causality between pathogen invasion and changes in rhizosphere microbiome composition

A separate greenhouse experiment was carried out to test whether pathogen invasion could change bacterial community composition and diversity under controlled environmental conditions. To this end, we used soil that was collected from a riverside in Zhangzhu town of Yixing, China (119°48′ 29″, 31°20′21″" - 160 km away from Nanjing) with no previous *R. solanacearum* infection history. Tomato seedlings were prepared as described above and 80 seedlings at similar growth stage were transplanted into plastic pots with 5 kg of sieved (at 5 mm) and homogenized dry soil. Ten plants were randomly selected and two rhizosphere soil samples per plant pooled together resulting in 5 initial rhizosphere soil samples. Subsequently, 35 plants were inoculated with *Ralstonia solanacearum* QL-Rs1115 strain (isolated from the field experimental site at Nanjing) by root drenching method resulting in final concentration of 5.0×10^6 CFU of bacteria g^{-1} soil (Pathogen present treatment). Another 35 plants were treated with the same amount of heat-killed (autoclaved at 121 °C for 20 min) suspension of dead *R. solanacearum* cells (Pathogen absent treatment). Tomato plants were then grown in a glass greenhouse with natural temperature variation ranging from 25 °C to 35 °C and watered regularly with sterile water for 32 days. The plant growth and disease development was monitored on daily basis. Subset of plants was sampled twenty days after the pathogen inoculation when the infected plants started to show visible disease symptoms. Briefly, three plants with functional root systems were harvested from both treatments at every two days for total of twelve days. Replicate samples within both treatments were then pooled at every sampling to result in 6 samples from the 'infected' and 6 samples from the 'control' treatment. All the final 17 rhizosphere soil

samples (including 5 initial samples) were stored at −80 °C for further analysis.

2.3. DNA extraction and sequencing

After digging out the plants, the excess root soil was removed gently by shaking and the remaining soil attached to roots (rhizosphere soil) chilled on ice before further storage at −80 °C. Total genomic DNA was isolated from the tomato rhizosphere soil (~0.25 g) by using PowerSoil DNA Isolation Kit (Mobio Laboratories, Carlsbad, CA, USA) following the manufacturer's protocol. DNA quality was checked on 1% agarose gel and DNA concentration was determined with NanoDrop 1000 spectrophotometer (Thermo Scientific, Waltham, MA, USA).

Bacterial community composition was characterized with multiplexed MiSeq sequencing. The V4 hypervariable region of the 16S rRNA gene was amplified with the primer pair 563F (5′-AYT GGG YDT AAA GVG-3′) and 802R (5′-TAC NVG GGT ATC TAA TCC-3′) (Cardenas et al., 2010). A barcode was attached to the forward primer and the reverse primer was combined to Y-shaped adapters allowing paired-end sequencing. Amplicons were purified by using magnetic bead sand, which was denatured with fresh NaOH. Denatured amplicons were sequenced by using a chip-based bridge amplification procedure, which synthesizes one nucleotide per each PCR cycle by using reversible terminator dye nucleotides. Reads were processed using the QIIME open-source bioinformatics pipeline (Caporaso et al., 2010). Briefly, sequences were removed if their lengths were shorter than 200 nt, their average quality score was < 20 and if they contained ambiguous bases, primer mismatches, homopolymer runs more than six bases or errors in the barcodes. Filtering of noisy sequences, chimera checking and operational taxonomic unit (OTU) cutoff was assigned at 97% identity level using the Usearch (Macdonald et al., 2011) pipeline and classified by using the RDP database with the online version of the RDP classifier (Margesin et al., 2011). *De novo* and reference-based chimera checking were performed, and sequences that were characterized as chimeric by both methods were removed. After filtering, on average 24769 (for the field samples, min = 9932, max = 47867) and 47119 (for the greenhouse samples, min = 36901, max = 57173) high-quality sequences per sample were obtained for subsequent analyses. The operational taxonomic unit (OTU) abundance of each sample was standardized by using the lowest number (9932 for the field samples and 36901 for the greenhouse samples) of sequence depth. The read count matrix was filtered by removing the OTUs with zero occurrences in all the samples. In the end, a total of 4814 field sample and 15060 greenhouse sample OTUs were retained for further analysis. Raw sequences were deposited into SequenceRead Archive database of NCBI SRA under the accession number SRP052295.

2.4. qPCR quantification of R. solanacearum densities

Ralstonia solanacearum densities were determined with qPCR by using primers targeting the *fliC* gene coding the flagella subunit (forward primer: 5′-GAA CGC CAA CGG TGC GAA CT-3′ and reverse primer: 5′-GGC GGC CTT CAG GGA GGT C-3′) (Schonfeld et al., 2003). The qPCR was carried out with Applied Biosystems 7500 Real-Time PCR System (Applied Biosystems, CA, USA) by using the SYBR Green I fluorescent dye detection in 20-µl volumes containing 10 µl of SYBR Premix Ex Taq (TaKaRa Biotech. Co, Japan), 2 µl of template, and 0.4 µl of both forward and reverse primers (10 mM each). The qPCR was performed by initially denaturing for 30 s at 95 °C with subsequent cycling for 40 times with a 5s denaturizing step at 95 °C. The protocol was followed by a 34s elongation/extension step at 60 °C and with a melt curve analysis for 15 s at 95 °C followed by 1 min at 60 °C and finally for 15 s at 95 °C. Melting curves were obtained based on a standard protocol and used to identify the characteristic peak of PCR product (400 bp). Four independent technical replicates were used for each sample.

2.5. Data analyses

2.5.1. Analysing changes in bacterial co-occurrence networks

Bacterial co-occurrence networks were inferred by using CoNet approach, a tool to detect significant non-random patterns of species co-occurrence in microbial incidence and abundance 16S rRNA sequencing data (Faust et al., 2012). Briefly, a matrix of read count of all OTUs in all samples, a matrix of environmental variables including soil pH, available phosphate, water-soluble carbon, water-soluble nitrogen, nitrate and ammonium, and a matrix of phylogeny lineage of all OTUs were uploaded. The read count matrix was filtered by keeping the OTUs with zero occurrence equal to 50% samples numbers. Pairwise associations between different OTUs were calculated by using Pearson, Spearman, Bray-Curtis and Kullback-Leibler correlations. Edges (i.e., species co-occurrence) supported by at least two correlation methods were retained. Initial top and bottom edge numbers were set at 2000. For each edge and each measure of association, 1000 permutation scores and 1000 bootstrap scores were computed. For the permutation of correlation measures, vectors of taxon pairs were first shuffled and then renormalized before computing scores to mitigate the compositional bias. Edge- and measure-specific p-values were determined as the area under the bootstrap distribution limited by the mean of the permutation distribution (see reference (Faust et al., 2012) for details on the p-value computation). Measure-specific p-values were then merged by using Brown's method and corrected for multiple testing with the Benjamini-Hochberg's procedure (Benjamini and Hochberg, 1995). Edges with scores outside the 95% confidence interval limit, defined by the bootstrap distribution or with adjusted p-values above 0.05, were discarded. A final network was restored from pre-computed permutation and bootstrap files and visualized in Cytoscape (Shannon et al., 2003). The differences between ‘initial’, ‘healthy’ and ‘diseased’ rhizosphere interaction networks were analysed by comparing various key topological network properties (the degree distribution, the network centralization values and the phylogenetic lineage of top hubs) and the presence and absence of certain interaction modules. The initial full networks and their key properties were calculated by using NetworkAnalyzer (Assenov et al., 2008) and OH-PIN algorithm (Wang et al., 2012) was used to construct co-occurrence sub networks (with positive edges only; threshold = 2; overlapping score = 0.5).

2.5.2. Analysing changes in predicted bacterial gene functions

The 16S rRNA sequencing data was further used to infer the abundance of functional genes with Phylogenetic Investigation of Communities by Reconstruction of Unobserved States (PICRUSt) (http://picrust.github.com/picrust/), a software package designed to infer metagenome functional content from 16S based OTU data (Langille et al., 2013). The paired-end merged 16S sequences were used for closed-reference OTU picking by using QIIME (Caporaso et al., 2010) version 1.6.0. The resulting OTU table was then fed into PICRUSt version 0.9.1 and functional predictions were made according to the metagenome inference workflow described by the developers (Langille et al., 2013).

2.5.3. Statistical analysis

All bacterial density data (OTU and qPCR) were log10 transformed and the relative pathogen abundance data (proportion of *R. solanacearum* OTU's of all bacterial OTU's) arcsine square root transformed before the statistical analysis. Bacterial community diversity was analysed by comparing the OTU richness of initial, healthy and diseased rhizosphere samples. All *R. solanacearum* OTUs were removed before this analysis to concentrate on changes in rhizosphere bacterial community composition. Analysis of partition of variance was further used to compare the relative importance of plant development (estimated as an effect of sampling time), physiochemical soil properties, rhizosphere bacterial community diversity (richness and Shannon index at OTU level) and community composition (at family level; *R. solanacearum*

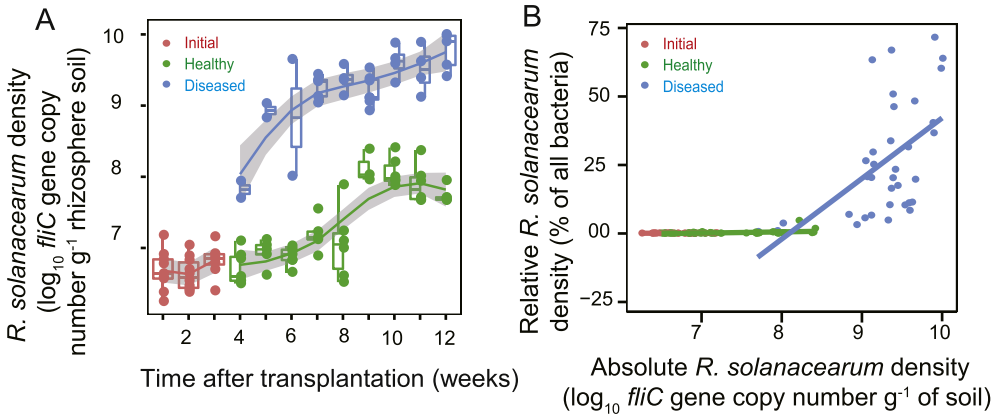

Fig. 1. *R. solanacearum* pathogen density dynamics during the field experiment. Panel **a**: Pathogen density dynamics in the rhizosphere samples during the crop season. Panel **b**: Relationship between the absolute and relative pathogen densities in tomato rhizosphere. In all panels, red, green and blue dots and lines denote for initially healthy, healthy and diseased tomato rhizosphere samples. (For interpretation of the references to colour in this figure legend, the reader is referred to the web version of this article.)

excluded) for the *R. solanacearum* density dynamics. ANOVA and non-parametric tests were used to compare the changes in bacterial taxa composition, the number of predicted gene functions and co-occurrence interaction network topologies.

3. Results

3.1. Disease development and R. solanacearum density dynamics during the field experiment

Ralstonia solanacearum pathogen could be detected in all rhizosphere soil samples since the beginning of the sampling even before any visible signs of bacterial wilt could be observed (pathogen density varying from $10^{6.25}$ to $10^{7.18}$ copy of *fliC* gene per gram of soil (Fig. 1A) – a number similar to viable cells isolated by plating count method (Wei et al., 2011). From week 4 on, we collected both visibly healthy and diseased plants that still had a functional root system (Figs. S1–B). *Ralstonia solanacearum* densities increased steadily throughout the crop season resulting in 10^{9}-10^{10} *fliC* gene copies per gram of soil in the diseased and 10^{7}-10^{8} *fliC* gene copies per gram of soil in the healthy plant samples by the end of the crop season ($P < 0.001$; Fig. 1A, Figs. S2–A). While the pathogen reached approximately 62.5-fold higher total abundances in the diseased compared to healthy rhizosphere samples (Fig. 1A, Figs. S2–A), the increase in the relative pathogen abundance was much higher (93.5-fold, $P < 0.001$; Figs. S2–B). The absolute and relative *R. solanacearum* densities correlated positively (Figs. S2–C) especially after reaching a threshold level of 10^{8}-$10^{8.5}$ copy *fliC* gene copies g^{-1} of dry soil in diseased samples (Fig. 1B).

3.2. Changes in the soil physiochemical properties during the field experiment

Of the six measured soil physiochemical properties only the phosphate availability showed non-significant changes during the crop season ($P = 0.051$, Fig. 2 and Fig. S3). In contrast, the amount of water-soluble nitrogen ($P < 0.001$) and the nitrate ($P = 0.005$) increased, while the concentrations of water-soluble carbon ($P < 0.001$), pH ($P < 0.001$) and ammonium ($P < 0.001$) decreased during the crop season (Fig. 2 and Fig. S3). This indicates that plant development (time) had clear effect on the dynamics of soil physiochemical properties. However, none of the physiochemical soil properties correlated significantly with pathogen densities in the diseased samples ($P > 0.12$ in all cases) and only the pH correlated significantly with pathogen densities in the healthy samples ($P = 0.023$; Table S1). Of all measured physiochemical properties, only the concentration of water-soluble nitrogen was slightly higher in the diseased plant samples and no difference was found in the case of other variables (Fig. 2).

3.3. Changes in the rhizosphere bacterial community composition and diversity during the field experiment

Both the plant development (time: $P < 0.001$, $F_{1,109} = 2.19$) and pathogen density ($P < 0.001$, $F_{1,109} = 2.79$) had strong effects on rhizosphere microbiome composition (Fig. 3A). Moreover, increase in pathogen densities was associated with reduced rhizosphere bacterial diversity (OTU richness, Fig. 3B) and high number of negative links with other bacteria in the diseased plant samples (Fig. 3C).

The density dynamics of the most abundant rhizosphere bacterial phyla differed significantly between the healthy and diseased samples (Fig. 3D–E). In general, the relative abundance of the Actinobacteria, Bacterioidetes, Chlorolflexi, Cyanobacteria, Firmicutes, Gemmatimonadetes, Planctomycetes, Verrucomicrobia and the unclassified group clearly decreased in the diseased compared to healthy plant samples (Fig. 3D–E). Crucially, no change was observed in the relative abundance of bacterial phyla between the initial and healthy samples (Fig. 3E), while half of the most abundant bacterial phyla showed a clear decrease in the diseased plant samples (Fig. 3E) including Actinobacteria, Chlorolflexi, Cyanobacteria, Gemmatimonadetes, Nitrospira, Planctomycetes and the unclassified group (similar trend also observed at the lower phylogenetic levels (Fig. S4). Clearest differences between the healthy and diseased rhizosphere samples were detected with *Chitinophagaceae* and *Bacillus* bacteria: both had clearly lower abundances in the diseased plant rhizosphere samples (Table S2).

3.4. Comparing the relative importance of abiotic and biotic factors for pathogen density dynamics during the field experiment

We found that changes in the rhizosphere bacterial community composition explained 20%, soil physiochemical properties only 1% and plant development (time) 13% of the total variation of pathogen density dynamics (Fig. 4). While changes in bacterial community composition correlated weakly with the soil physiochemical properties and the plant development explaining less than 1% of total variation (Fig. 4), interactive effects between plant development and soil physiochemical properties explained 36% of the total variation of pathogen density dynamics.

3.5. Comparing changes in the rhizosphere bacterial co-occurrence networks during the field experiment

To gain further insight into bacterial community development during the crop season, we constructed bacterial co-occurrence networks for the initial, healthy and diseased plants and compared their key topological properties (Fig. 5 and Fig. S5). The networks differed regarding their degree distribution, centralization values, and the phylogenetic lineage of the top hubs (particularly the top hubs with negative links, Fig. 5). The degree distribution of the initial and healthy

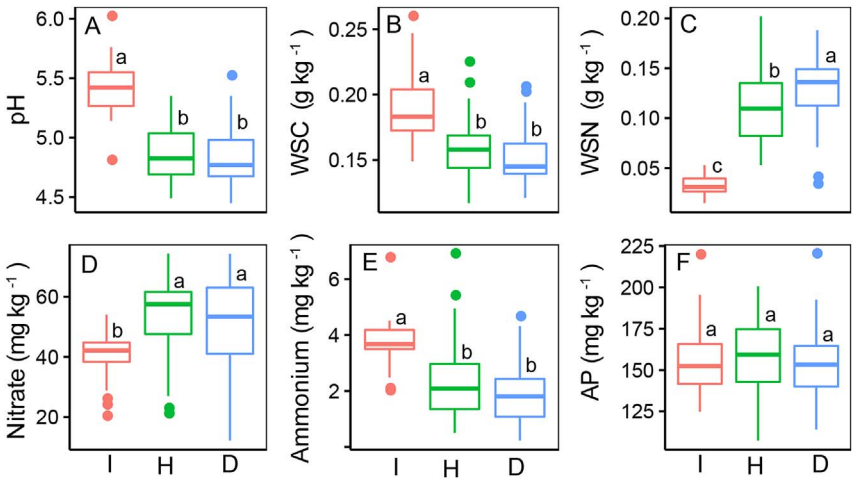

Fig. 2. Differences in the physiochemical soil properties during the field experiment. Panel **a-f**: Differences in mean physiochemical soil properties between initial (I, red), healthy (H, green), and diseased (D, blue) plant rhizosphere samples (averaged over time). The WSC denotes for water soluble carbon, WSN for water soluble nitrogen, AP for available phosphate, NO_3^- for nitrate and NH_4^+ for ammonium. Lowercase letters within the panels denote for statistical difference at the level of $P < 0.05$. (For interpretation of the references to colour in this figure legend, the reader is referred to the web version of this article.)

plant networks had high exponential values (-value = 1.072–1.125) and followed well the power-law with the number of network nodes (R^2-values ~0.84, Fig. 5). In contrast, the number of nodes of diseased plant networks had poorer fit (R^2-value ~0.54, Fig. 5) and did not scale exponentially with the degree distribution (-value = 0.665) indicative of scale-free topology. Centralization values showed a similar trend. As for the top hub, nodes belonging to Alpha-proteobacteria were consistently predicted as positively-linked hubs across all the networks (Fig. 5). However, the negatively-linked hubs were different for all the networks: while Acidobacteria had the highest number of negative links in the initial network, Actinobacteria and Alpha-proteobacteria had the highest number of negative links in the healthy and diseased plant networks, respectively (Fig. 5). These data suggest that the initial bacterial co-occurrence networks were more similar to healthy compared to diseased plant samples.

In the case of co-occurrence subnetwork modules, total of 13 and 16

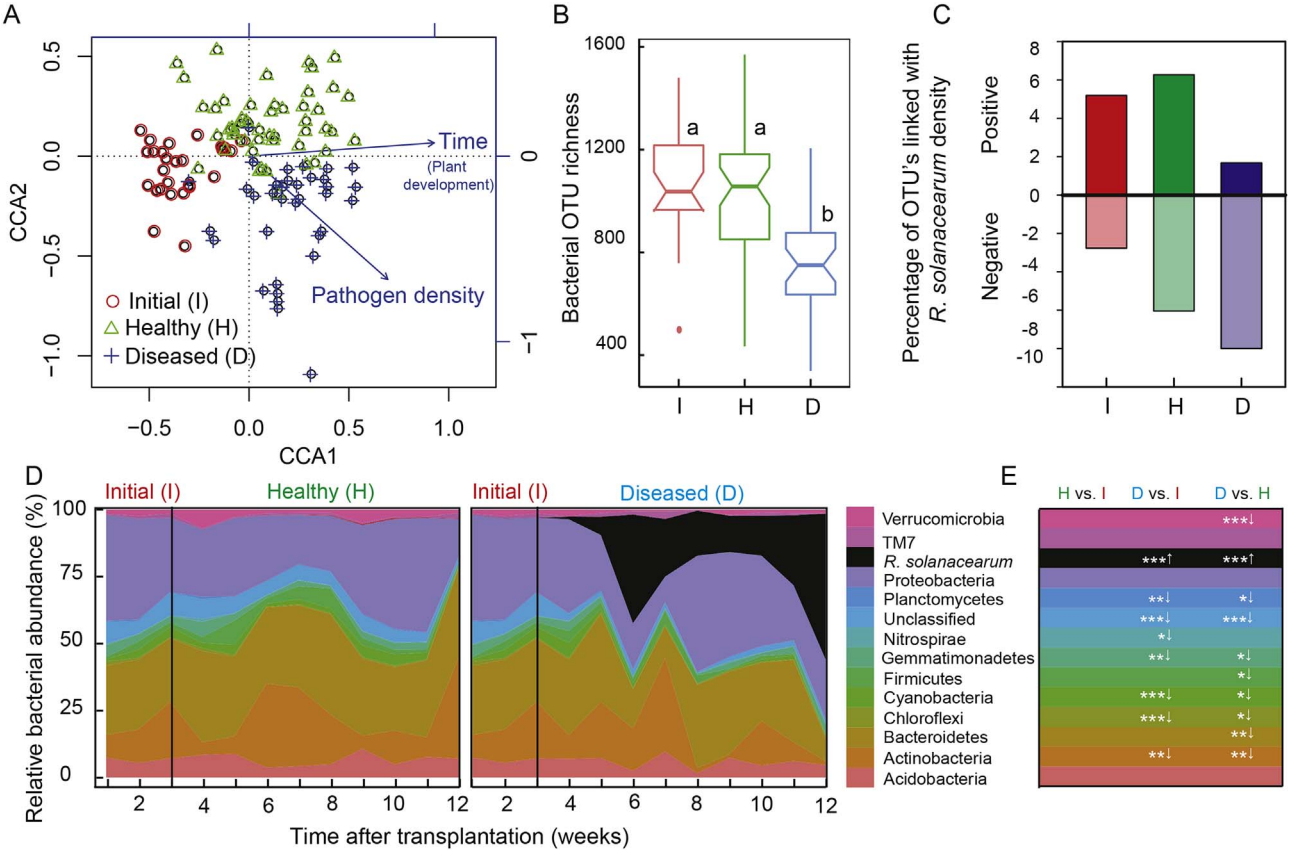

Fig. 3. Changes in the rhizosphere microbiome composition and diversity during the field experiment. Panel **a**: The effect of time (plant development) and pathogen density changes on the rhizosphere microbiome composition. Panel **b**: The differences in bacterial community richness (number of OTU) in initial, healthy and diseased plant rhizosphere samples. Panel **c**: The percentage of significant ($P < 0.05$) bacterial OTUs that were positively or negatively linked with *R. solanacearum* densities. Panel **d**: The relative bacterial density dynamics (*R. solanacearum* in black and other bacterial phyla with different colors) in initial, healthy and diseased plant rhizosphere samples (number of OTU). Panel **e**: The comparison different bacterial phyla abundance between initial and healthy plant rhizosphere samples (H vs. I), initial and diseased plant rhizosphere samples (D vs. I) and healthy and diseased plant rhizosphere samples (D vs. H; *, ** and *** represent significances at $P < 0.05$, $P < 0.01$ and $P < 0.001$ levels, respectively; downward and upward arrows denote for decrease and an increase in the bacterial abundances of the first group relative to the second group, respectively). (For interpretation of the references to colour in this figure legend, the reader is referred to the web version of this article.)

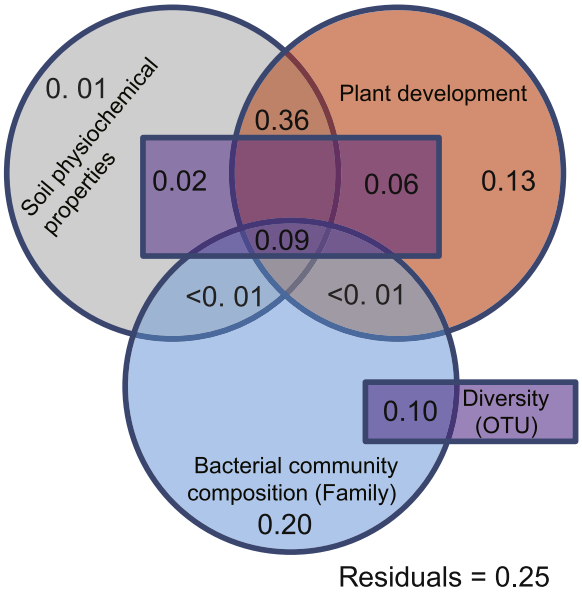

Fig. 4. Partition of variance analysis explaining the correlation between the total pathogen density changes with changes in the soil physiochemical properties, time (plant development), rhizosphere bacterial community composition (at family level) and diversity (Shannon diversity index at OTU level).

modules were predicted for initial and healthy networks, while only 9 modules were predicted for the diseased network (Fig. 5). Some of the modules were unique and detected only in one of the sample group, while other modules showed overlap and were detected in two or every sample groups (Fig. S5). The healthy network had higher similarity to the initial network (44% and 22% module overlap for healthy vs. initial and diseased vs. initial comparisons, respectively) even though healthy network modules were often more complex than the initial network modules. Second, diseased network modules were generally less complex and had less interacting species compared to initial and healthy network modules (Fig. S5). Moreover, overlap between initial and diseased network modules was mainly found when the same modules overlapped also between the initial and healthy networks (Fig. S5). Together these results suggest that pathogen invasion correlated with reduced number and complexity of bacterial co-occurrence sub-networks more clearly in the diseased rhizosphere samples.

3.6. Correlating pathogen invasion with the abundance of predicted functional genes during the field experiment

We found that COG modules (a group of protein-encoding genes performing similar or the same function) of almost all functional gene classes changed mainly in the diseased rhizosphere sample group (Table S3 and Table S4). Only the loss of gene functions was detected and these were mostly connected with translation, energy production and conversion, and transport and bacterial metabolism (Table S3 and Table S4). Interestingly, only few inferred gene functions correlated with pathogen densities in healthy rhizosphere samples (Fig. S6). In contrast, inferred functional gene abundances correlated mostly negatively with pathogen densities in the diseased rhizosphere samples (Fig. S6).

3.7. Verifying the causal relationship between pathogen invasion and changes in microbiome composition in a greenhouse experiment

The pathogen *R. solanacearum* successfully invaded tomato rhizosphere with a high relative abundance after 20–30 days post inoculation (Fig. 6A). Similar to field sampling, both the plant development and the presence of pathogen had clear effects on bacterial community composition in tomato rhizosphere (comparison between initial, pathogen and control treatments, Fig. 6B). The initial samples had clearly the highest bacterial richness compared to both pathogen and control treatments (Fig. 6C). Crucially, bacterial richness was the lowest in the presence of pathogen compared to control treatment (Fig. 6C). Consistent with the field experiment, the abundances of Verrucomicrobia, Gemmatimonadetes, Cyanobacteria and Chlorolflexi were significantly lower in the presence of the pathogen (Fig. 6D). Furthermore, the abundance of Nitrospirae and Acidobacteria decreased in the presence of pathogen in the greenhouse experiment (Fig. 6D). Plant development had also strong effect on rhizosphere bacterial community development in the absence of pathogen (Fig. 6B). Together these results confirm that pathogen invasions can causally reduce the rhizosphere microbiome bacterial abundance and richness.

4. Discussion

Here we studied how soil physiochemical properties, plant development (time) and bacterial community composition interact and correlate with *R. solanacearum* invasion success in tomato plant rhizosphere under natural field conditions in China. Our results show that pathogens were found at low abundances in all rhizosphere samples in the beginning of the field experiment. While the soil physiochemical properties showed clear temporal patterns with the plant development, no clear correlation was observed with the disease incidence or pathogen densities. In contrast, pathogen densities correlated strongly with a community-wide shift in the bacterial community composition in the diseased rhizosphere samples leading to almost 100-fold decrease in the relative abundance of non-pathogenic rhizosphere bacteria. This drastic shift in microbiome composition correlated with loss of diversity across different taxonomic levels, simplification of bacterial co-occurrence interaction networks and reduction in the abundance of predicted functional genes. Qualitatively very similar results were found also in a separate greenhouse experiment. Together these results suggest that *R. solanacearum* invasions can drive community-wide shifts in rhizosphere microbiome composition and functioning irrespective of soil physiochemical properties.

Even though most soil physiochemical properties showed clear temporal changes during the crop season, only minor differences were found between healthy and diseased samples. Furthermore, temporal changes in soil physiochemical properties correlated weakly with pathogen densities but strongly with plant development (i.e., time). The pH, water-soluble carbon and ammonium concentration decreased during the plant development. While pH and concentrations of carbon and ammonium have previously been shown to have direct effects on the *R. solanacearum* (Dalsing and Allen, 2014; Li et al., 2017; Yang et al., 2017), we found that, pathogen densities increased in time regardless of lowered pH and available carbon. Crucially, soil physiochemical properties did not differ between healthy and diseased samples, which suggest that they unlikely affected, or were driven, by disease dynamics. Instead, abiotic changes were likely driven by plant development and were generally at benign range for *R. solanacearum* growth. Only physiochemical property that correlated positively with disease dynamics was the concentration of water-soluble nitrogen. Nitrate availability is important for the *R. solanacearum* virulence gene expression during the attachment and colonization of tomato plant roots and xylem (Dalsing et al., 2015; Dalsing and Allen, 2014) and could thus have affected pathogen virulence without having a considerable effect on the pathogen density.

Ralstonia solanacearum was found in similar absolute and relative abundances in all sample groups in the beginning of the field experiment. Correspondingly, all the sampled rhizosphere bacterial communities were similar in their composition in the beginning of the field experiment. However, the relative abundance of non-pathogenic rhizosphere bacteria clearly decreased in the diseased soil samples towards the end of the experiment. Clear decline was found in the relative abundances of Actinobacteria, Bacterioidetes, Chlorolflexi,

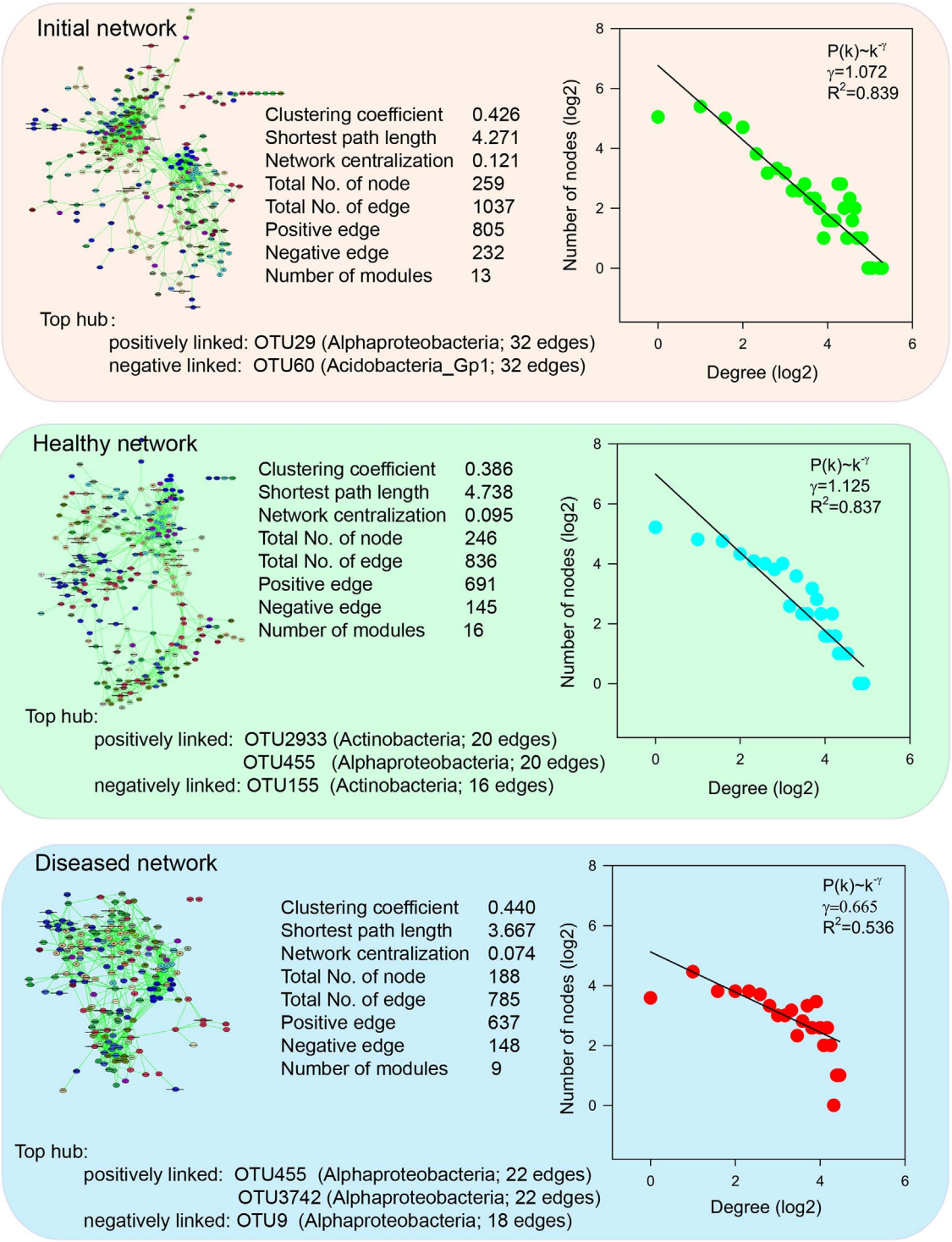

Fig. 5. The comparison of bacterial co-occurrence network properties between initial, healthy and diseased plant rhizosphere samples. Difference in network properties of the initial, healthy and diseased plant rhizosphere samples.

Cyanobacteria, Firmicutes, Gemmatimonadetes, Planctomycetes and Verrucomicrobia. These compositional changes could have affected, or be a consequence of, pathogen density dynamics during the invasion. For example, reduction in the relative abundance of *Actinobacteria* that produce over two-thirds of the clinically useful antibiotics (Procopio et al., 2012) could have had a positive effect on the *R. solanacearum* growth due to weakened pathogen suppression via antibiosis (Yuliar et al., 2015). We also saw a clear reduction in the abundance of Bacteroidetes phylum, particularly with the species from *Chitinophagaceae* family and *Bacillus* genera that are also known for their antagonistic activity (lipopeptide antibiotics) against *R. solanacearum* (Wei et al., 2011). Bacteria from *Chitinophagaceae* have previously been associated with soil communities with high β-glucosidase activity (Bailey et al., 2013), which is indicative of bacterial ability to break down cellulose (indicative of efficient carbon turnover). *Chitinophagaceae* could thus have promoted bacterial diversity by increasing the number of available nutrients from the dead plant biomass. We also observed a clear reduction in the abundance of many functionally important genes and

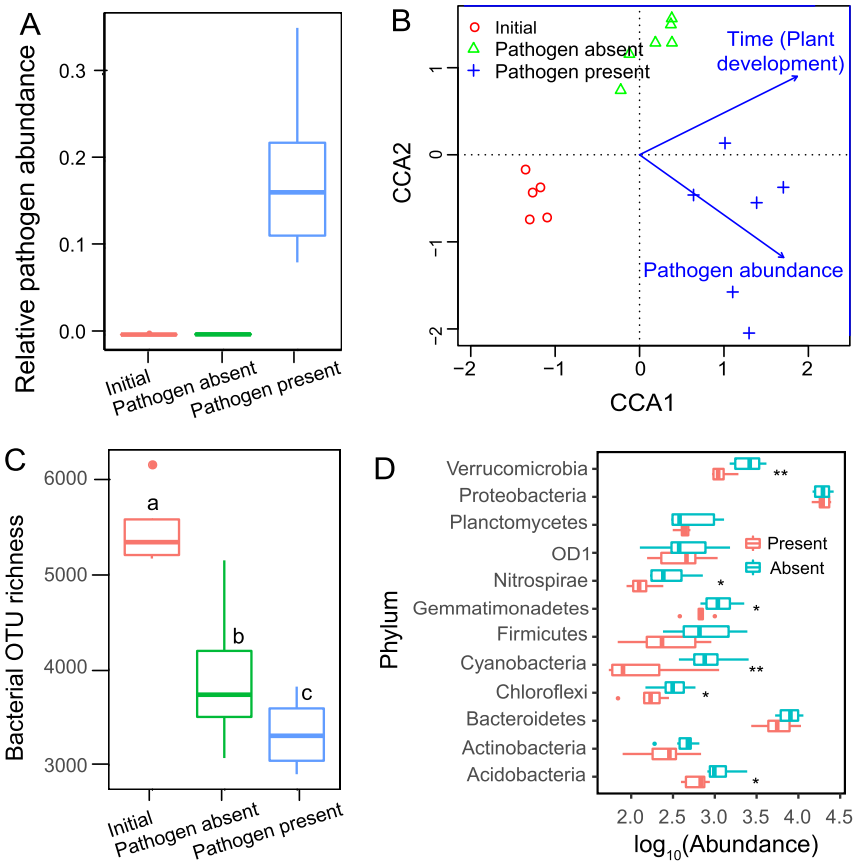

Fig. 6. The effect of pathogen presence and time (plant development) on rhizosphere microbiome composition and diversity during separate greenhouse experiment. Panel **a**: Relative pathogen abundance in the tomato rhizosphere. Panel **b**: Time (plant development) and pathogen presence had strong effects on the bacterial community composition. Panel **c**: The effect of pathogen presence and time (plant development) on the richness of rhizosphere bacterial microbiome (OTU level). Different letters denote for statistical a difference at the level of $P < 0.05$. Panel **d**: The differences in bacterial abundance at phylum level between pathogen absent and present treatments; * and ** denotes for statistical a difference at the level of $P < 0.05$ and $P < 0.01$, respectively. Initial, pathogen present and pathogen absent refer to the three treatment groups described in Materials and Methods section.

simplification of bacterial co-occurrence networks in terms of reduced network complexity and loss of various sub-network modules. Together these findings suggest that the loss of diversity correlated with loss of microbiome functioning potentially leading to loss of functions related to pathogen suppression. However, it is not clear why aggressive pathogen invasions were linked with decreased abundance of potential antibiotic-producing bacteria. One potential explanation for this could be that intensified resource competition favoured pathogen growth with the expense of antibiotic-producing bacteria (Hu et al., 2016). Alternatively, trophic interactions with predators and parasites could have had more negative effect on antibiotic-producing bacteria compared to the pathogen (Jousset et al., 2010, 2009; Wang et al., 2017b). Further work is needed to understand these results more mechanistically.

Disruption of host-associated microbiomes during pathogen invasion has been observed before with pathogenic fungi (Chapelle et al., 2016; Walke and Belden, 2016). For example, Chapelle et al. (2016) used metagenomics approach to link the fungal invasions with elevated expression of bacterial stress related genes, which could have caused changes in microbiome composition directly or indirectly by changing plant root exudation. Similarly, fungal invasion has been connected to highly predictable and consistent changes in frog skin microbiome (Walke and Belden, 2016). Together these findings suggest that while high microbial diversity has previously been linked to strong invasion resistance (Elsas et al., 2012; Hu et al., 2016; Wei et al., 2015), pathogens can also trigger drastic changes in the microbiome composition leading to loss of diversity and predicted community functioning. This kind of feedback loops could be very important for long-term disease dynamics. For example, in the context of agriculture, once-invaded rhizosphere communities could become more susceptible to secondary invasions during following crops seasons leading to downward spiral of recurrent infections. Moreover, the strong negative correlation between pathogen and non-pathogenic bacterial densities suggest that relative pathogen abundance could better predict the severity of bacterial wilt disease outbreaks compared to absolute pathogen abundance. Monitoring the pathogen dynamics relative to the changes in the surrounding microbiome could thus open new avenues for developing more accurate disease diagnostics in the future.

Because it is not possible to separate cause and consequence based on the field sampling data, we conducted a controlled small-scale greenhouse experiment to directly study how pathogen presence shapes the rhizosphere microbiome composition. Consistent with the field experiment, plant development (time) and the pathogen presence had clear effects on rhizosphere microbiome composition and diversity. Crucially, pathogen presence led to highest reduction in bacterial community richness relative to initial community composition. While we observed similar changes in the abundances of key bacterial phyla between field and greenhouse experiments in general, some groups responded differently. This is likely explained by the inherent differences between the pathogen and rhizosphere bacterial communities (field vs. river bank soil) and the controlled experimental design (absence or presence of one single pathogen). Regardless of these small differences, patterns between field and greenhouse experiments were qualitatively very similar demonstrating a causal link between *R. solanacearum* invasion and rhizosphere microbiome change. One potential mechanism behind this is pathogen-mediated change in plant exudation (Gu et al., 2016). Recently, Gu et al. (2016) showed with tomato that *R. solanacearum* presence can trigger changes in the exudation of different phenolic compounds and caffeic acid. In line with our results, the root exudates from pathogen-infected plants led to development of less diverse rhizosphere bacterial communities, while increased exudation of caffeic acid had direct negative effects on the invading pathogen (Gu et al., 2016). Together these results suggest that both the amount and composition of secreted tomato root exudates could have changed in response to *R. solanacearum* invasion leading to disruption of rhizosphere microbiome community.

Despite the good match between field and greenhouse experiment, it is still unclear why pathogen could infect only some plants in the field even though it was initially present everywhere. One explanation could be that the healthy and diseased plant rhizosphere samples showed temporal variation in the onset of disease: sampled diseased plants could have been infected earlier, while sampled healthy plants would have become infected at later stage. However, only 50% of all the plants got infected during the crop season, which suggest that some plants remained healthy throughout the field experiment. Another explanation is that soil-borne pathogens, such as *R. solanacearum*, might exist in bimodal alternative stable states being very rare or very abundant in the rhizosphere (Lahti et al., 2014). For example, the abundances of bimodally distributed gut bacteria are not affected by the short-term dietary interventions (Lahti et al., 2014), but instead, the contrasting alternative states are associated with gradual long-term changes with host ageing and the development of obesity (Lahti et al., 2014). Even though we did not find clear linear correlations between soil physiochemical properties and the pathogen densities, it is possible that small gradual changes in environmental conditions or composition of bacterial taxa could have shaped the microbiome assembly during the initial phases of plant development. This could have onset disease development and pathogen invasion in some rhizosphere communities, for example, via density-mediated threshold (Fig. 1). Further complications could have risen from our prokaryotic-centric approach, which did not consider the effects of predatory protists, nematodes, parasitic bacterial viruses or competing fungi on the relative abundance of the pathogen (Addy et al., 2012; Jogaiah et al., 2013; Jousset et al., 2009; Vandenkoornhuyse et al., 2015). For example, lipopeptides produced by *R. solanacearum* have been shown to trigger formation of resting spores with 34 fungal species, which suggest that bacterial wilt outbreaks could indirectly affect fungal survival (Spraker et al., 2016). Future work should thus focus on looking beyond prokaryotes during *R. solanacearum* invasions. Moreover, we did not control for the intraspecific genetic variation of the pathogen or explored if pathogen could have evolved regarding its infectiveness during the field experiment (Guidot et al., 2014; Riley et al., 2001). Further research is thus still needed to fully understand the complexity of *R. solanacearum* infections in the field conditions.

In conclusion, here we show that *R. solanacearum* infection dynamics are associated with a drastic reduction in rhizosphere microbiome abundance, composition and diversity irrespective of soil physiochemical properties. These results suggest that *R. solanacearum* invasions could potentially disrupt the functioning of rhizosphere bacterial community and that the relative *R. solanacearum* abundance might be a better indicator of the onset of bacterial wilt outbreak instead of absolute pathogen abundance. It however remains unclear why *R. solanacearum* infections are patchy under seemingly homogenous field conditions and to what extent the loss of diversity affects the functioning of rhizosphere microbiome such as resistance to secondary invasions and plant growth promotion. More detailed fine-scale metagenomics, sequencing data and bacteria-plant responses and communication via root exudates will hopefully help to elucidate the causal drivers of bacterial wilt disease outbreaks in the future.

Acknowledgements

We thank Lucas William Mendes and Jens Bast for the suggestion of data analysis. This research was financially supported by the National Key Basic Research Program of China (2015CB150503), the National Natural Science Foundation of China (41471213 and 41071117), the Natural Science Foundation of Jiangsu Province (BK20170085), the 111 project (B12009), and the Young Elite Scientist Sponsorship Program by CAST (2015QNSC001). Ville-Petri Friman is supported by the Wellcome Trust [ref: 105624] through the Centre for Chronic Diseases and Disorders at the University of York. Jie Hu is supported by the joint PhD scholarship of Chinese Scholarship Council.

Appendix A. Supplementary data

Supplementary data related to this article can be found at http://dx.doi.org/10.1016/j.soilbio.2017.11.012.

References

Addy, H.S., Askora, A., Kawasaki, T., Fujie, M., Yamada, T., 2012. Utilization of filamentous phage phi RSM3 to control bacterial wilt caused by Ralstonia solanacearum. Plant Disease 96, 1204–1209. http://dx.doi.org/10.1094/Pdis-12-11-1023-Re.

Assenov, Y., Ramirez, F., Schelhorn, S.E., Lengauer, T., Albrecht, M., 2008. Computing topological parameters of biological networks. Bioinformatics 24, 282–284. http://dx.doi.org/10.1093/bioinformatics/btm554.

Bailey, V.L., Fansler, S.J., Stegen, J.C., Mccue, L.A., 2013. Linking microbial community structure to beta-glucosidic function in soil aggregates. Isme Journal 7, 2044–2053. http://dx.doi.org/10.1038/ismej.2013.87.

Benjamini, Y., Hochberg, Y., 1995. Controlling the false discovery rate - a practical and powerful approach to multiple testing. Journal of the Royal Statistical Society Series B-methodological 57, 289–300.

Caporaso, J.G., Kuczynski, J., Stombaugh, J., Bittinger, K., Bushman, F.D., Costello, E.K., Fierer, N., Pena, A.G., Goodrich, J.K., Gordon, J.I., Huttley, G.A., Kelley, S.T., Knights, D., Koenig, J.E., Ley, R.E., Lozupone, C.A., McDonald, D., Muegge, B.D., Pirrung, M., Reeder, J., Sevinsky, J.R., Tumbaugh, P.J., Walters, W.A., Widmann, J., Yatsunenko, T., Zaneveld, J., Knight, R., 2010. QIIME allows analysis of high-throughput community sequencing data. Nature Methods 7, 335–336. http://dx.doi.org/10.1038/nmeth.f.303.

Cardenas, E., Wu, W.M., Leigh, M.B., Carley, J., Carroll, S., Gentry, T., Luo, J., Watson, D., Gu, B.H., Ginder-Vogel, M., Kitanidis, P.K., Jardine, P.M., Zhou, J.Z., Criddle, C.S., Marsh, T.L., Tiedje, J.M., 2010. Significant association between sulfate-reducing bacteria and uranium-reducing microbial communities as revealed by a combined massively parallel sequencing-indicator species approach. Applied and Environmental Microbiology 76, 6778–6786. http://dx.doi.org/10.1128/Aem.01097-10.

Chaparro, J.M., Badri, D.V., Vivanco, J.M., 2014. Rhizosphere microbiome assemblage is affected by plant development. The ISME Journal 8, 790–803. http://dx.doi.org/10.1038/ismej.2013.196.

Chapelle, E., Mendes, R., Bakker, P.A.H., Raaijmakers, J.M., 2016. Fungal invasion of the rhizosphere microbiome. The ISME Journal 10, 265–268. http://dx.doi.org/10.1038/ismej.2015.82.

Dalsing, B.L., Allen, C., 2014. Nitrate assimilation contributes to Ralstonia solanacearum root attachment, stem colonization, and virulence. Journal of Bacteriology 196, 949–960. http://dx.doi.org/10.1128/JB.01378-13.

Dalsing, B.L., Truchon, A.N., Gonzalez-Orta, E.T., Milling, A.S., Allen, C., 2015. Ralstonia solanacearum uses inorganic nitrogen metabolism for virulence, ATP production, and detoxification in the oxygen-limited host xylem environment. Mbio 6. http://dx.doi.org/10.1128/mBio.02471-14.

Denny, T.P., Baek, S.R., 1991. Genetic-evidence that extracellular polysaccharide is a virulence factor of pseudomonas-solanacearum. Molecular Plant-microbe Interactions 4, 198–206. http://dx.doi.org/10.1094/Mpmi-4-198.

Elsas, J.D. van, Chiurazzi, M., Mallon, C.A., Elhottovā, D., Krištůfek, V., Salles, J.F., 2012. Microbial diversity determines the invasion of soil by a bacterial pathogen. Proceedings of the National Academy of Sciences 109, 1159–1164. http://dx.doi.org/10.1073/pnas.1109326109.

Elsas, J.D. van, Kastelein, P., de Vries, P.M., van Overbeek, L.S., 2001. Effects of ecological factors on the survival and physiology of *Ralstonia solanacearum* bv. 2 in irrigation water. Canadian Journal of Microbiology 47, 842–854. http://dx.doi.org/10.1139/cjm-47-9-842.

Faust, K., Sathirapongsasuti, J.F., Izard, J., Segata, N., Gevers, D., Raes, J., Huttenhower, C., 2012. Microbial Co-occurrence relationships in the human microbiome. PLOS Computational Biology 8, e1002606. http://dx.doi.org/10.1371/journal.pcbi.1002606.

Genin, S., Denny, T.P., 2012. Pathogenomics of the Ralstonia solanacearum species complex. Annual Review of Phytopathology 50, 67–89. http://dx.doi.org/10.1146/annurev-phyto-081211-173000.

Gu, Y., Wei, Z., Wang, X., Friman, V.-P., Huang, J., Wang, X., Mei, X., Xu, Y., Shen, Q., Jousset, A., 2016. Pathogen invasion indirectly changes the composition of soil microbiome via shifts in root exudation profile. Biology and Fertility of Soils 52, 997–1005. http://dx.doi.org/10.1007/s00374-016-1136-2.

Guidot, A., Jiang, W., Ferdy, J.B., Thebaud, C., Barberis, P., Gouzy, J., Genin, S., 2014. Multihost experimental evolution of the pathogen Ralstonia solanacearum unveils genes involved in adaptation to plants. Molecular Biology and Evolution 31, 2913–2928. http://dx.doi.org/10.1093/molbev/msu229.

Hayward, A.C., 1991. Biology and epidemiology of bacterial wilt caused by Pseudomonas solanacearum. Annual Review of Phytopathology 29, 65–87. http://dx.doi.org/10.1146/annurev.py.29.090191.000433.

Hibbing, M.E., Fuqua, C., Parsek, M.R., Peterson, S.B., 2010. Bacterial competition: surviving and thriving in the microbial jungle. Nature Reviews Microbiology 8, 15–25. http://dx.doi.org/10.1038/nrmicro2259.

Hu, J., Wei, Z., Friman, V.-P., Gu, S., Wang, X., Eisenhauer, N., Yang, T., Ma, J., Shen, Q., Xu, Y., Jousset, A., 2016. Probiotic diversity enhances rhizosphere microbiome function and plant disease suppression. MBio 7http://dx.doi.org/10.1128/mBio.01790-16. e01790–16.

Huang, J.F., Wei, Z., Tan, S.Y., Mei, X.L., Yin, S.X., Shen, Q.R., Xu, Y.C., 2013. The rhizosphere soil of diseased tomato plants as a source for novel microorganisms to

control bacterial wilt. Applied Soil Ecology 72, 79–84. http://dx.doi.org/10.1016/j.apsoil.2013.05.017.
Huang, Q., Allen, C., 2000. Polygalacturonases are required for rapid colonization and full virulence of Ralstonia solanacearum on tomato plants. Physiological and Molecular Plant Pathology 57, 77–83. http://dx.doi.org/10.1006/pmpp.2000.0283.
Jiang, G.F., Wei, Z., Xu, J., Chen, H.L., Zhang, Y., She, X.M., Macho, A.P., Ding, W., Liao, B.S., 2017. Bacterial wilt in China: history, current status, and future perspectives. Frontiers in Plant Science 8. http://dx.doi.org/10.3389/Fpls.2017.01549.
Jogaiah, S., Abdelrahman, M., Tran, L.S., Shin-ichi, I., 2013. Characterization of rhizosphere fungi that mediate resistance in tomato against bacterial wilt disease. Journal of Experimental Botany 64, 3829–3842. http://dx.doi.org/10.1093/jxb/ert212.
Jousset, A., Becker, J., Chatterjee, S., Karlovsky, P., Scheu, S., Eisenhauer, N., 2014. Biodiversity and species identity shape the antifungal activity of bacterial communities. Ecology 95, 1184–1190. http://dx.doi.org/10.1890/13-1215.1.
Jousset, A., Rochat, L., Pechy-Tarr, M., Keel, C., Scheu, S., Bonkowski, M., 2009. Predators promote defence of rhizosphere bacterial populations by selective feeding on non-toxic cheaters. Isme Journal 3, 666–674. http://dx.doi.org/10.1038/ismej.2009.26.
Jousset, A., Rochat, L., Scheu, S., Bonkowski, M., Keel, C., 2010. Predator-prey chemical warfare determines the expression of biocontrol genes by rhizosphere-associated Pseudomonas fluorescens. Applied and Environmental Microbiology 76, 5263–5268. http://dx.doi.org/10.1128/AEM.02941-09.
Lahti, L., Salojarvi, J., Salonen, A., Scheffer, M., de Vos, W.M., 2014. Tipping elements in the human intestinal ecosystem. Nature Communications 5. http://dx.doi.org/10.1038/Ncomms5344.
Langille, M.G.I., Zaneveld, J., Caporaso, J.G., McDonald, D., Knights, D., Reyes, J.A., Clemente, J.C., Burkepile, D.E., Thurber, R.L.V., Knight, R., Beiko, R.G., Huttenhower, C., 2013. Predictive functional profiling of microbial communities using 16S rRNA marker gene sequences. Nature Biotechnology 31http://dx.doi.org/10.1038/nbt.2676. 814–+.
Li, S., Liu, Y., Wang, J., Yang, L., Zhang, S., Xu, C., Ding, W., 2017. Soil acidification aggravates the occurrence of bacterial wilt in South China. Frontiers in Microbiology 8. http://dx.doi.org/10.3389/fmicb.2017.00703.
Li, Y., Sun, H., Li, H., Yang, L., Ye, B., Wang, W., 2013. Dynamic changes of rhizosphere properties and antioxidant enzyme responses of wheat plants (Triticum aestivum L.) grown in mercury-contaminated soils. Chemosphere 93, 972–977. http://dx.doi.org/10.1016/j.chemosphere.2013.05.063.
Macdonald, C.A., Clark, I.M., Zhao, F.J., Hirsch, P.R., Singh, B.K., McGrath, S.P., 2011. Long-term impacts of zinc and copper enriched sewage sludge additions on bacterial, archaeal and fungal communities in arable and grassland soils. Soil Biology & Biochemistry 43, 932–941. http://dx.doi.org/10.1016/j.soilbio.2011.01.004.
Mallon, C.A., Poly, F., Le Roux, X., Marring, I., van Elsas, J.D., Salles, J.F., 2015. Resource pulses can alleviate the biodiversity-invasion relationship in soil microbial communities. Ecology 96, 915–926. http://dx.doi.org/10.1890/14-1001.1.
Margesin, R., Plaza, G.A., Kasenbacher, S., 2011. Characterization of bacterial communities at heavy-metal-contaminated sites. Chemosphere 82, 1583–1588. http://dx.doi.org/10.1016/j.chemosphere.2010.11.056.
Mendes, R., Kruijt, M., de Bruijn, I., Dekkers, E., van der Voort, M., Schneider, J.H.M., Piceno, Y.M., DeSantis, T.Z., Andersen, G.L., Bakker, P.A.H.M., Raaijmakers, J.M., 2011. Deciphering the rhizosphere microbiome for disease-suppressive bacteria. Science (New York, N.Y) 332, 1097–1100. http://dx.doi.org/10.1126/science.1203980.
Piotrowska-Dlugosz, A., Lemanowicz, J., Dlugosz, J., Spychaj-Fabisiak, E., Gozdowski, D., Rybacki, M., 2016. Spatio-temporal variations of soil properties in a plot scale: a case study of soil phosphorus forms and related enzymes. Journal of Soils and Sediments 16, 62–76. http://dx.doi.org/10.1007/s11368-015-1180-9.
Procopio, R.E.D., da Silva, I.R., Martins, M.K., de Azevedo, J.L., de Araujo, J.M., 2012. Antibiotics produced by streptomyces. Brazilian Journal of Infectious Diseases 16, 466–471. http://dx.doi.org/10.1016/j.bjid.2012.08.014.
Riley, M.S., Cooper, V.S., Lenski, R.E., Forney, L.J., Marsh, T.L., 2001. Rapid phenotypic change and diversification of a soil bacterium during 1000 generations of experimental evolution. Microbiology-sgm 147, 995–1006.
Saile, E., McGarvey, J.A., Schell, M.A., Denny, T.P., 1997. Role of extracellular polysaccharide and endoglucanase in root invasion and colonization of tomato plants by Ralstonia solanacearum. Phytopathology 87, 1264–1271. http://dx.doi.org/10.1094/Phyto.1997.87.12.1264.
Schell, M.A., 2000. Control of virulence and pathogenicity genes of Ralstonia solanacearum by an elaborate sensory network. Annual Review of Phytopathology 38, 263–292. http://dx.doi.org/10.1146/annurev.phyto.38.1.263.
Schonfeld, J., Heuer, H., van Elsas, J.D., Smalla, K., 2003. Specific and sensitive detection of Ralstonia solanacearum in soil on the basis of PCR amplification of fliC fragments. Applied and Environmental Microbiology 69, 7248–7256. http://dx.doi.org/10.1128/Aem.69.12.7248-7254.2003.
Shannon, P., Markiel, A., Ozier, O., Baliga, N.S., Wang, J.T., Ramage, D., Amin, N., Schwikowski, B., Ideker, T., 2003. Cytoscape: a software environment for integrated models of biomolecular interaction networks. Genome Research 13, 2498–2504. http://dx.doi.org/10.1101/gr.1239303.
Shi, S., Nuccio, E., Herman, D.J., Rijkers, R., Estera, K., Li, J., Rocha, U.N. da, He, Z., Pett-Ridge, J., Brodie, E.L., Zhou, J., Firestone, M., 2015. Successional Trajectories of Rhizosphere Bacterial Communities over Consecutive Seasons. MBio 6http://dx.doi.org/10.1128/mBio.00746-15. e00746–15.
Spraker, J.E., Sanchez, L.M., Lowe, T.M., Dorrestein, P.C., Keller, N.P., 2016. Ralstonia solanacearum lipopeptide induces chlamydospore development in fungi and facilitates bacterial entry into fungal tissues. ISME Journal. http://dx.doi.org/10.1038/ismej.2016.32.
van Elsas, J.D., Kastelein, P., de Vries, P.M., van Overbeek, L., 2001. Effects of ecological factors on the survival and physiology of Ralstonia solanacearum bv. 2 in irrigation water. Canadian Journal of Microbiology 47, 842–854.
Vandenkoornhuyse, P., Quaiser, A., Duhamel, M., Le Van, A., Dufresne, A., 2015. The importance of the microbiome of the plant holobiont. New Phytologist 206, 1196–1206. http://dx.doi.org/10.1111/nph.13312.
Walke, J.B., Belden, L.K., 2016. Harnessing the microbiome to prevent fungal infections: lessons from Amphibians. PLOS Pathogens 12, e1005796. http://dx.doi.org/10.1371/journal.ppat.1005796.
Wang, H., Wei, Z., Mei, L., Gu, J., Yin, S., Faust, K., Raes, J., Deng, Y., Wang, Y., Shen, Q., Yin, S., 2017a. Combined use of network inference tools identifies ecologically meaningful bacterial associations in a paddy soil. Soil Biology and Biochemistry 105, 227–235. http://dx.doi.org/10.1016/j.soilbio.2016.11.029.
Wang, J.X., Ren, J., Li, M., Wu, F.X., 2012. Identification of hierarchical and overlapping functional modules in PPI networks. Ieee Transactions on Nanobioscience 11, 386–393. http://dx.doi.org/10.1109/Tnb.2012.2210907.
Wang, X., Wei, Z., Li, M., Wang, X., Shan, A., Mei, X., Jousset, A., Shen, Q., Xu, Y., Friman, V.-P., 2017b. Parasites and competitors suppress bacterial pathogen synergistically due to evolutionary trade-offs. Evolution 71, 733–746. http://dx.doi.org/10.1111/evo.13143.
Wei, Z., Huang, J., Yang, T., Jousset, A., Xu, Y., Shen, Q., Friman, V.-P., 2017. Seasonal variation in the biocontrol efficiency of bacterial wilt is driven by temperature-mediated changes in bacterial competitive interactions. Journal of Applied Ecology. http://dx.doi.org/10.1111/1365-2664.12873. n/a-n/a.
Wei, Z., Yang, T., Friman, V.-P., Xu, Y., Shen, Q., Jousset, A., 2015. Trophic network architecture of root-associated bacterial communities determines pathogen invasion and plant health. Nature Communications 6, 8413. http://dx.doi.org/10.1038/ncomms9413.
Wei, Z., Yang, X., Yin, S., Shen, Q., Ran, W., Xu, Y., 2011. Efficacy of Bacillus-fortified organic fertiliser in controlling bacterial wilt of tomato in the field. Applied Soil Ecology 48, 152–159. http://dx.doi.org/10.1016/j.apsoil.2011.03.013.
Yabuuchi, E., Kosako, Y., Yano, I., Hotta, H., Nishiuchi, Y., 1995. Transfer of two burkholderia and an alcaligenes species to Ralstonia gen. Nov.: proposal of Ralstonia pickettii (ralston, palleroni and doudoroff 1973) comb. Nov., Ralstonia solanacearum (smith 1896) comb. Nov. and Ralstonia eutropha (davis 1969) comb. Nov. Microbiology and Immunology 39, 897–904.
Yang, T., Wei, Z., Friman, V.-P., Xu, Y., Shen, Q., Kowalchuk, G.A., Jousset, A., 2017. Resource availability modulates biodiversity-invasion relationships by altering competitive interactions. Environmental Microbiology. http://dx.doi.org/10.1111/1462-2920.13708. n/a-n/a.
Yuliar, Nion, Y.A., Toyota, K., 2015. Recent trends in control methods for bacterial wilt diseases caused by Ralstonia solanacearum. Microbes and Environments 30, 1–11. http://dx.doi.org/10.1264/jsme2.ME14144.